

Distributed electric propulsion with blended wing-body for fixed-wing UAVs

Daniel Castroviejo, Maximilien Van Der Stichelen** and Patrick Hendrick****

**ULB, Aero-Thermo-Mechanics department, Brussels, Belgium*

daniel.castroviejo@ulb.be

*** ULB, Aero-Thermo-Mechanics department, Brussels, Belgium*

maximilien.van.der.stichelen@ulb.be

****ULB, ULB, Aero-Thermo-Mechanics head of department, Brussels, Belgium*

Abstract

In the quest for sustainable aviation, Distributed Propulsion (DP) might offer many advantages. For this technology, ducted propellers are investigated to increase efficiency and aerodynamic performance of an aircraft. DP offers some advantages as improved maneuverability, control surfaces area reduction, boundary layer ingestion capability and even more. In this paper, EDF (Electric Ducted Fans) will be presented, with an analysis of the effect of the duct on the propeller efficiency that will be quantified. A test bench equipped with high resolution sensors has been built to effectively test, measure and analyze these EDFs for electric drones. It is found that a duct can be able to increase up to 43% the thrust or reduce the power consumption by 62%. DP really appear as a viable choice towards cleaner aviation but EDFs now need to be integrated in the plane's structure to limit the parasitic drag they add.

1. Introduction

The last 50 years have seen an incredible increase in the number of passengers transported by plane annually. When aviation really started to gain popularity and the theoretical/technical skills were developed, companies were always aiming at building bigger and faster planes such as the notorious concorde or the boeing 747 released respectively in 1976 and 1989. However, since then a lot of things have changed, among them is the chase towards a cleaner planet, with good air quality and a healthy environment. To do so, all sectors must find new and innovant ways to keep their activities ongoing while being as environmentally friendly as possible. Aviation is no exception, thus, reducing consumption and emissions of aircrafts is one of the primary concerns in the aeronautical sector today. One of the possible ways towards reducing the fuel consumption is to increase the aircraft's performance and that might be one of the advantages Distributed Propulsion (DP) may have to offer [1].



Figure 1.1: Skywalker X8 UAV

This paper will treat of DP for a Skywalker X8 (SX8), a Blended Wing-Body (BWB) aircraft which can be seen on Figure 1.1. It is an Unmanned Aerial Vehicle (UAV) measuring 2.12m wingspan and the focus is on improving the control authority and performances of such an aircraft. As will be seen later, some Electric Ducted Fan (EDF) will be used which have a specific behavior (e.g. the transients will be much shorter than for big planes fans) but this does not prevent from applying the results here in the aviation sector. The goal is not exactly the same either, but it aligns with aviation goals to reduce emissions: what must be optimized is the endurance of this drone which employs an electric battery as power supply. For this kind of small drone, increasing the endurance of just a few minutes is already a great improvement. However even though the final aim is to fully explore the benefits of DP, this paper focuses on the

testbench used and the effect of the presence of the duct around the EDFs (the results can be scaled up using non-dimensional numbers theory).

2. State-of-the-art

To be able to discuss DP it is important to have a clear definition of what it really is, it is defined in this paper as “the spanwise distribution of the propulsive thrust stream such that overall, the vehicle benefits in terms of aerodynamic, propulsive, structural and/or other efficiencies to enhance the vehicle mission” [2]. This type of technology can bring many benefits, listed here below.

Increased Lift capabilities: As the motors suck more air on the low-pressure part of the wing this has for effect to further reduce the pressure and thus increase the lift allowing for wing area reduction or increased lift capabilities [1].

Boundary Layer Ingestion (BLI): By embedding the engines into the aircraft’s structure, they can ingest the boundary layer. This allows first of all for a reduced drag on the engine as part of the exposed surface of the engine to the free flow forms now part of the plane. Simultaneously the drag on the aircraft itself is reduced as part of that drag is ingested by the fan [9]. Additionally, as a portion of the fan absorbs a slower velocity flow (the boundary layer) the fan has to produce less work for the same thrust (see equation 3.3 where v_{jet} and v_a can be replaced respectfully by v_{out} and v_{in} , being the fan outlet and inlet velocities) [10]. What is challenging here is that the boundary layer is a highly disturbed flow and thus it affects the propeller’s efficiency. Hence specific propellers designed to withstand such conditions while being efficient at the same time are being developed [9].

Increased control authority: By placing various motors along the wingspan of the aircraft, differential thrust is able to enhance the control authority of the aircraft. This leads to more compact control surfaces or even to the absence of control surfaces, allowing for weight reduction. It can also possibly decrease drag while performing maneuvers by decreasing control surfaces deflection.

Relieving bending stresses: Due to a more homogeneous distribution of the motors along the wingspan the load is evenly distributed and eventually this allows a decrease in the wing’s structure weight.

2.2 Hunting H.126

An example of a plane using a type of DP system is the British hunting H.126 developed in the early sixties which made its first flight in March 1963, built by Hunting aircraft for purely research purposes [3]. The technology they used is known as jet flaps, consisting of bleeding air from the engine and redirecting it through the fuselage all the way to the wings (which is thus considered to be part of DP as it is the redirection of the engine thrust along the wingspan). This type of propulsion allowed the aircraft to fly at speeds as low as 51 km/h [4] as well as decreasing take-off and landing distances.

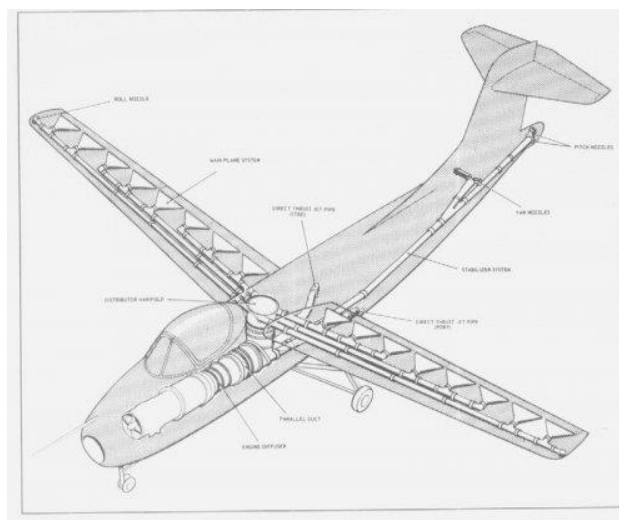


Figure 2.1: Schematic of the Hunting H.126

This aircraft was powered by a single Bristol Siddeley Orpheus turbojet engine [3] and more than 50% of the engine thrust is redirected along 16 jets distributed evenly along the wingspan, these allowed for increased lift, explaining

how it could be maintained in the air at such low speeds. Additional jets were placed on the tail of the aircraft to control pitch and yaw movements and on the wingtips to control roll. These were added specifically to increase the manoeuvrability of the aircraft at low speeds since the aerodynamic forces exerted on the control surfaces is minor, such a plane can be seen on Figure 2.1.

2.3 Ampere

A promising concept plane that the French society Office National d'Etudes et de Recherches Aérospatiales (ONERA) has been developing is known as the AMPERE [5] (from french: "Avion à Motorisation réPartie Electrique de Recherche Expérimentale", basically meaning it is a DP research plane). It uses a distributed electric propulsion system with motors evenly distributed along the wingspan and should be capable of transporting up to 6 persons within a 500 km range. One of their aims is to build an optimal propulsion system while keeping the drag on the plane as low as possible. To do so their project aims to use EDFs. Indeed, the concept plane is built such that 32 independent motors are installed on its wings. These electric motors are to be powered by 8 hydrogen fuel cells. ONERA has planned for different configurations of the plane. One consists of top mounted wings with leading edge EDFs whereas the other is a low mounted wing with canard configuration positioning the EDFs on the trailing edge of the wings, both configurations visible in Figure 2.2.

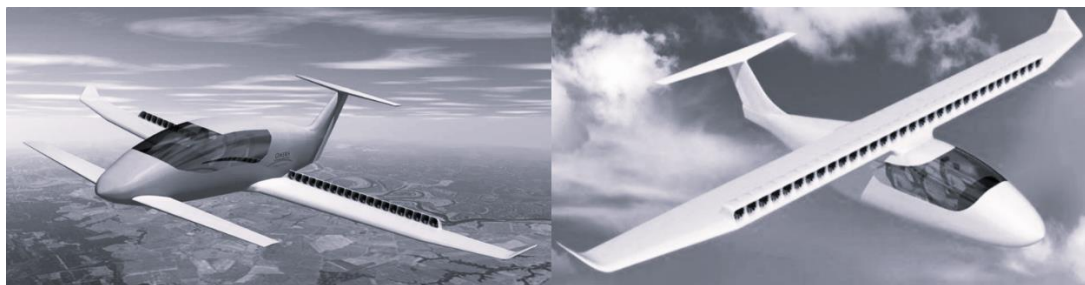


Figure 2.2: ONERA concept plane, AMPERE

No published results have been found concerning the aerodynamic performance of the AMPERE but a wind tunnel testing on a one fifth scaled model has already been shown in a Paris conference with some interesting results regarding the boundary layer attachment on the airfoil, allowing for greater performance.

3. Material, methodology and results

The goal of the project was to realize some test flights on the SX8 equipped with its basic propulsion configuration, which consists of a single 30 cm diameter propeller in pusher configuration. By doing so it is possible to analyze its flight envelope and aerodynamic characteristics such as take-off speed, stall speed, autonomy, power consumption and more. To do so, the BWB aircraft was equipped with a Pixhawk cube orange flight controller (known to be reliable with redundant gyroscopes and accelerometers [1]), a GPS for the auto pilot, movement tracking and ground speed as well as a pitot tube to calculate the air speed.

After performing a complete analysis on the said drone and having run a thorough investigation on the EDFs, the aim was to mount a distributed electric propulsion system, based on previous calculations, and quantify the benefits brought by such a system. Unfortunately, this goes beyond the scope of this paper. Thus, only the study of the motor performance will be shown and explained here.

3.2 EDF presentation

It is deemed useful to expose the motors characteristics used in this project. Note that what is known as an EDF is the assembly of an electric motor, a propeller and a duct. For the electric motors, mainly the maximum deliverable power and the Kv's of the motors are important parameters. The Kv is an indication on the motor's maximum rotational speed. Indeed, by multiplying the latter parameter with the motors applied external voltage (thus the voltage of the battery used, usually it is possible to use different voltage levels on one motor), the maximum rotational speed of the motor with the given power source is obtained. The higher the Kv usually the smaller the motor. All of the studied motors are small as they are to be equipped on a drone and their specifications are shown in Table 3.1. Furthermore

Figure 3.1 shows a picture of the JP 70 EDF such as to have a clear image of the EDFs used, note that this motor was the highest performance motor used which came in full aluminum casing and propeller.

Table 3.1: EDFs used and their specifications

| EDF | Kv | I_{\max} [A] | V_{\max} [V] | RPM _{max} | Thrust _{max} [g] | Weight [g] | Duct diameter [mm] |
|-------------|-------|----------------|----------------|--------------------|---------------------------|------------|--------------------|
| QX-3300 | 3300 | 45 | 16.8 | 55 500 | 750 | 77 | 50 |
| QX-3500 | 3500 | 55 | 16.8 | 58 800 | 1250 | 142 | 64 |
| QX-4500 | 4500 | 27 | 12.6 | 56 700 | 750 | 84 | 64 |
| Racestar 40 | 7000 | 25 | 12.6 | 88 200 | 450 | 48 | 40 |
| QX-14000 | 14000 | 12 | 8.4 | 117 600 | 215 | 21 | 30 |
| JP 70 | 2250 | 88 | 25.2 | 56 700 | 2350 | 225 | 70 |



Figure 3.1: JP 70 EDF, full aluminum

3.1 The Testbench

In order to be able to study the effect of the duct on the propulsive force and the consumed power, it is mandatory to have a fully functional and reliable test bench. Hence, a test bench was built in order to be able to measure different physical variables of the tested motors. The testbench was built and equipped with throttle, torque, thrust, rpm, current, voltage, temperature, static and dynamic pressure sensors. All of the data is then collected and processed by an Arduino Mega board and sent to a Raspberry Pi from which it is transferred to MATLAB where it is treated and analyzed, a schematic of the testbench can be seen in Figure 3.2. Before exploiting the results of the test bench, it is important to validate the measurements taken by the data acquisition system. For the following parameters (rotational speed, voltage, current and thus power), the measurements have been compared to those of the Scorpion Tribunus I. Indeed, this high-quality ESC is equipped with various internal sensors allowing for the latter parameters to be recorded and thus compared to those of the test bench, with a relatively high definition and sampling rate. The comparison, even though chosen not to be shown here, shows a good working condition of the test bench. With an increasing sampling frequency, the difference between both acquisition system seems to reduce.

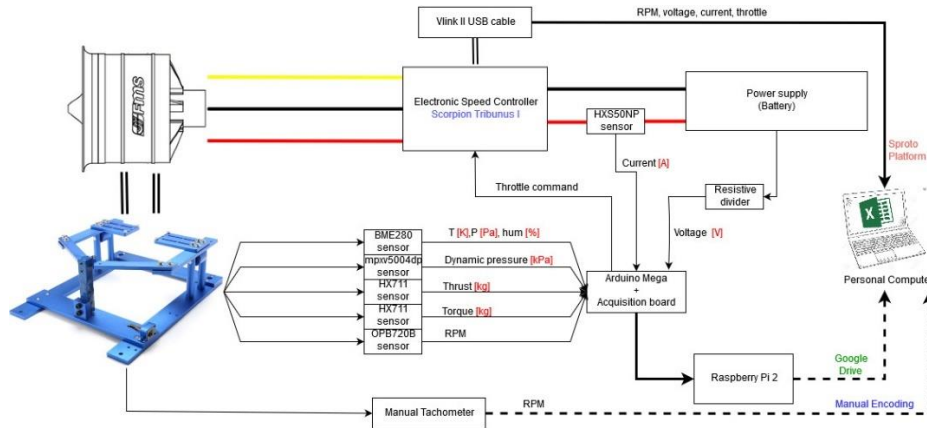


Figure 3.2: Acquisition scheme of the testbench

3.3 Mass flow and thrust computations

First Approximation. Once it is certain that the measured variables are correct, it is deemed interesting to compare the experimentally measured thrust (through means of a force sensors) versus the computed thrust (based on different physical variables such as air density ρ , dynamic pressure p_{dyn} and blade swept area A) to further corroborate the used equipment. But in order to calculate the thrust, the mass flow is needed (\dot{m}) which depends on the air density, the outlet section flow velocity v_{jet} of the propeller and the blade swept area. Indeed, the total mass flow rate is computed with the continuity equation as figured in Equation 3.1.

$$\dot{m} = \rho v_{jet} A \quad (3.1)$$

The velocity at the exit of the propeller will be determined by help of a pitot tube sensor. By placing it just behind the fan and inside the duct, the dynamic pressure at the fan outlet section is retrieved and will then be used to compute the flow velocity. Using Bernoulli's equation leads to Equation 3.2.

$$v_{jet} = \left(\frac{2p_{dyn}}{\rho} \right)^{1/2} \quad (3.2)$$

Then by injecting the found velocity into Equation 3.1 the physical mass flow of air flowing through the duct is found. The value of ρ chosen both in Equations 3.1 and 3.2 is computed using the perfect gas law with the ambient room temperature and pressure. Indeed, the effects of the fan flow on the atmospheric conditions are negligible [1] for these kinds of motors and thus the actual room conditions measured at the beginning of the tests can be used. Once the mass flow is computed, the propulsive force noted as F can be too. The thrust can be computed with Equation 3.3 which is the general equation of the generated thrust of a turbojet engine [7]. Note that as we are on a testbench and thus in static conditions, the aircraft speed (v_a) is null.

$$F = \dot{m}(v_{jet} - v_a) \quad (3.3)$$

Applying the explained methodology just above on the QX4500, some plots are drawn. The flow velocity increases linearly with the rotational speed, as it was to be expected. It is important to note that the maximum flow speed reached for the biggest EDF (JP 70) tested at maximum power is equal to 65 m/s. Computing the speed of sound and dividing the speed by the latter (shown in Equation 3.4, where γ is the adiabatic index, R the molar gas constant and T the absolute temperature), it is found that the highest Mach number reached is 0.25. This Mach number being below 0.3 allows to state that compressibility effects are negligible throughout the rest of the study.

$$M = \frac{v_{jet}}{(\gamma RT)^{1/2}} \quad (3.4)$$

For the two obtained thrusts in function of the rpm, a graph with two different curves is obtained and a clear deviation can be seen between both curves, see figure 3.3. The experimental thrust is always lower than the expected theoretical

thrust and by a non-negligible amount. After examination of the experiment, it was determined this was due to the fact that the mass flow is not precisely determined. Indeed, by computing the mass flow as explained earlier, the boundary layer of the flow is not considered (or the velocity profile distribution along the radius) and as the EDF's carter radius's quite small, this boundary layer omission has a non-negligible impact on the EDF flow. Indeed, for the QX4500, the biggest difference in thrusts reached is $\Delta F = 1017 - 650 = 367 \text{ g}$, yielding an overshoot error of 56 %, which is far too much. It would thus be interesting to determine the boundary layer height and hence the velocity profile inside the duct.

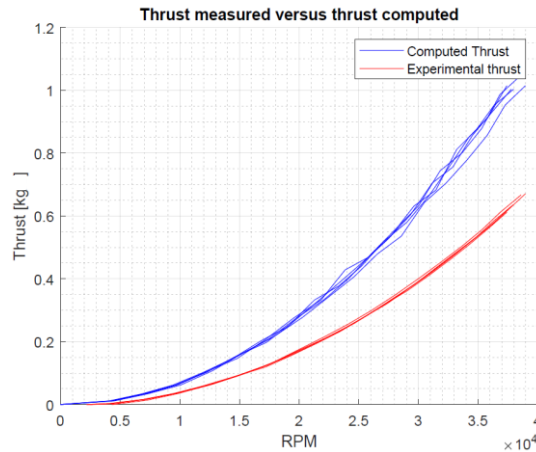


Figure 3.3: Thrust comparison for QX4500, first approximation

Second approximation. In this part, tests were made in order to have a complete and precise velocity distribution inside the duct. The thrust when calculated using the flow velocity, mass flow and density was overestimated compared to the one that was measured. Due to the presence of the boundary layer where the flow has a reduced velocity, one can expect a reduction of the computed thrust as well and the results are to be closer to the real thrust. The tests were made using a precision pitot tube holder designed in the study. The pitot was placed at a fixed position on the x-axis to be inside the duct between the fan outlet section and the duct outlet section. On the z-axis, it was also placed at a fixed position: at the same height as the center of the motor. That leaves only one degree of freedom: the y axis, along which the velocity was measured. Moving the pitot tube mm by mm, 16 data points were acquired, two extra points were added using one basic assumption: the no-slip condition which states that for viscous fluids, at a solid boundary, the fluid velocity is null [8]. Figure 3.4 shows the experimental velocity distribution scattered in blue (for throttle position).

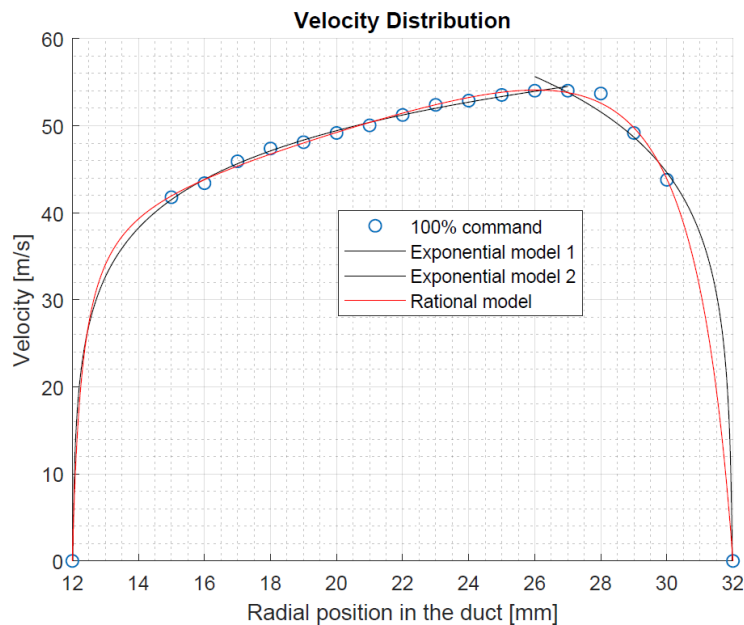


Figure 3.4: Velocity profile in the duct

In order to integrate this velocity distribution, a linear interpolation did not seem the best option, thus different curve fits were studied using Matlab. First, following the theory of fluid mechanics inside smooth pipes [8], a logarithmic model 1 was used and the data had to be separated in two boundary layers: a boundary layer close to the center of the EDF and one close to the duct that gave two models, the equations are not shown here. These models correspond to the black curves shown in figure 3.4. Another model was found to fit very well the data points but without any physical meaning behind: the rational model, shown in red in figure 3.4. Once the velocity distribution has been found the mass flow and thrust can be computed using an integration along the radius, yielding equations 3.5 and 3.6.

$$\dot{m} = \int_{12}^{32} 2 \times 10^{-6} \pi \rho v_{jet}(r) dr \quad (3.5)$$

$$F = \int_{12}^{32} 2 \times 10^{-6} \pi \rho v_{jet}^2(r) dr \quad (3.6)$$

In these equations r is the radius in mm. Using the rational velocity distribution gives a mass flow of 146 g/s and a thrust of 719 g compared to a value given by the force sensor of 650g, thus giving an overshoot error of 10%, much better than in the first approximation. It can be concluded that refining the velocity distribution instead of using a single value of the velocity at the center of the duct gives results for the thrust that are much closer to the real variable. Of course, the remaining error on the thrust might come from different sources (curve fitting model, sensors precision) but what must also be considered is that the force sensor measures the resulting force $F_{measured} = F_{real} - F_{drag}$. However, while using the velocity distribution only the thrust term is computed, and it seems thus logical that a higher value is found when comparing to the experimental thrust since the induced drag on the duct/motor has not been accounted.

3.3 Duct effect on thrust and power

Many factors influencing the EDF's performance have been treated in detail throughout the study, such as for instance the influence of the battery charge/discharge and the blade profile on its performance, the electronic speed controller's impact on the control of the EDF and much more. The most interesting results deemed for this paper are the impact of the duct on the thrust production and power consumption. These are shown here in Figure 3.5 (where EUF stands for Electric Unducted Fans, which is basically a simple propeller) for two different EDFs (the QX3300 and QX4500). The two different colors represent each of the motors. The full lines are with the duct mounted whereas the dotted lines represent the propeller without a duct.

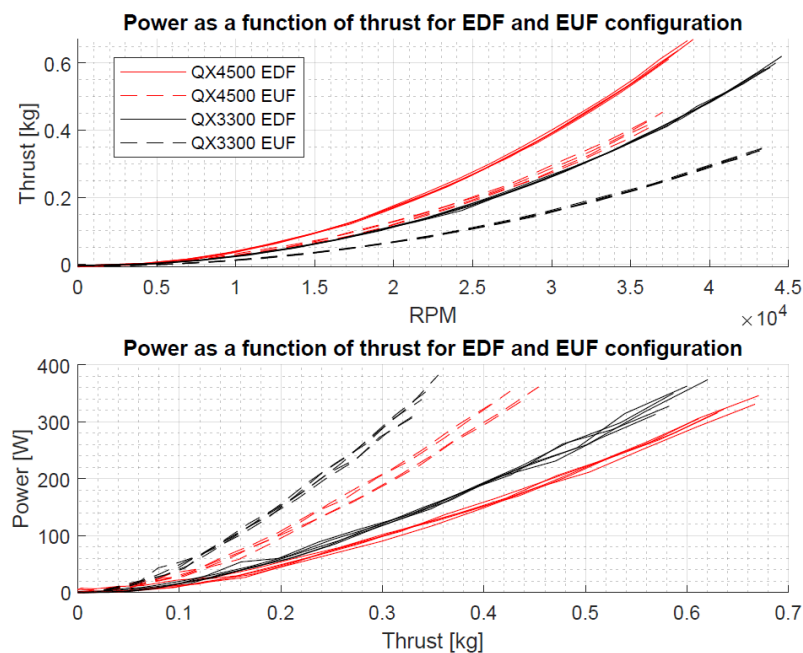


Figure 3.5: Thrust and power graphs

For each of these motors, exactly the same propeller was used, only the presence of the duct changes. The short analysis will be conducted on the QX3300, thus all values given here concern the black lines, similar conclusions can be drawn for other motors. Note that each curve overlaps pretty well with 4 others, this is because for each configuration 5 tests were performed for redundancy.

With just a quick glance at the results, the positive impact of the duct is clearly visible. From this figure it can be seen that installing a duct around the propeller allows for a much higher thrust production, the higher the thrust the bigger the difference. For the QX3300, at maximum rpm, the thrust varies from 355g to 620g for respectively the unducted and ducted motors, corresponding to an increase of 43%, this is huge. Looking at the bottom graph of figure 3.5, the power consumed by the motor as a function of the thrust produced is exposed. Again, looking at the black lines, for the maximum thrust of the propeller without duct, the motor equipped with the latter uses 210W less, resulting in a decrease of power consumption of 62%, again this is an impressive enhancement of the propeller's performance. These improvements are due to the more uniform flow established beneath the propeller and the disappearance or decrease of blade tip vortices by installing the duct, allowing for a higher efficiency of the fan. It is important to notice that the increase in parasitic drag due to the presence of the duct has not been studied and this is an important parameter which will be integrated in future work of the project.

3. Conclusions

It is now clear that the use of distributed propulsion (DP) can offer some great advantages for fixed wing UAVs. Amongst them is the famous BLI, which seems to offer a consistent drag reduction and to decrease the fan power consumption [10], along with other advantages such as increased control authority for the UAV and a reduced structural (dry) mass.

Furthermore, the presence of the duct increases consequently the static (non-installed) thrust of a given propeller in EDFs. Moreover, for the same thrust, the power consumption is also considerably reduced. This clearly shows an improvement in the performance of propellers when being equipped with a duct (the different parameters of this duct are yet to be studied).

The benefits from combining DP and EDFs is now clearer and will be further studied. When implementing DP on an aircraft, whether it is a drone or a manned aircraft, it is mandatory to place the engine such as they are embedded in the fuselage/wing structure to minimize the added drag and take advantage of BLI.

References

- [1] Daniel Castroviejo, Maximilien Van Der Stichelen, Patrick Hendrick, 2020. Distributed electric propulsion for drones (UAVs) in the ULB facilities. In: Master thesis ULB, ULB, Brussels.
- [2] Hyun Dae Kim., Distributed Propulsion Vehicles in NASA Glenn research centre. In: 27th International Congress of the Aeronautical Sciences, ICAS 2010.
- [3] James Felder, Hyun Kim and Gerald Brown, June 2012. Turboelectric Distributed Propulsion Engine Cycle Analysis for Hybrid-Wing-Body Aircraft in NASA Glenn research center. In: Session: FD-42: Progress Toward Hybrid Wing Body II.
- [4] "Hunting H.126 Jet-Flap Research Aircraft: Details of the British Aircraft Corporation Research Aircraft Designed to a Ministry of Aviation Specification Which Recently Made its First Flight". In: Aircraft Engineering and Aerospace Technology, Vol. 35 No. 6, pp. 166-167.
- [5] AMPERE, the distributed electric propulsion challenge, in ONERA report, 2017.
- [6] James L. Felder. 2014. NASA N3-X with turboelectric distributed propulsion.
- [7] Patrick Hendrick, 2019. Aircraft propulsion, ULB course, ULB, Brussels.
- [8] Gérard Degrez, 2018. MECA-H-305 Fluids Mechanics II, ULB course, ULB, Brussels.
- [9] NASA, November 2019. Boundary layer ingestion propulsion in Aeronautics. In: NASA Glenn research centre. <https://www1.grc.nasa.gov/aeronautics/bli/>
- [10] Budziszewski N, Friedrichs J., 2018. Modelling of A Boundary Layer Ingesting Propulsor. In: Energies 11(4):708.